Small-Angle X-ray Scattering Study on the Conformation of Polystyrene in Compressed CO_2−Tetrahydrofuran Mixtures

Dan Li,[†] Zhimin Liu,[†] Buxing Han,*[,†] Guanying Yang,[†] Zhonghua Wu,[‡] Yi Liu,[‡] and Baozhong Dong[‡]

Center for Molecular Sciences, Institute of Chemistry, Chinese Academy of Science, Beijing 100080, China, and Institute of High Energy Physics, Chinese Academy of Science, Beijing 100039, China

Received May 17, 2000; Revised Manuscript Received August 1, 2000

ABSTRACT: Cloud points of the compressed CO_2 + tetrahydrofuran (THF) + polystyrene (PS) system was studied at temperature range of 298.15−328.15 K and at different pressures. The expansion of the solution caused by dissolved CO_2 was also studied. Synchrotron radiation small-angle X-ray scattering (SAXS) was used to investigate the dissolved CO_2 on the conformation of PS. The second virial coefficient A_2 and the apparent mean-square radius of gyration $\langle R_g^2 \rangle^{1/2}$ at different pressures were obtained. It was found that the PS chain shrinks with increasing the concentration of CO_2.

Introduction

Supercritical fluids (SCFs) are becoming an increasingly important solvent system for use in polymer science and engineering.[1] Supercritical CO_2, in particular, is a widely used solvent due to its low cost, moderate critical conditions, and environmentally benign nature. However, only amorphous fluoropolymers and silicones are found to be soluble in supercritical CO_2 at relatively mild conditions,[2−5] while most polymers and many other solutes are not soluble in it.

High-pressure gases, especially CO_2, are quite soluble in a number of organic solvents and expand them largely at pressures ranging from 1.0 to 10.0 MPa,[6] which can reduce the solvent strength to such an extent that a solid dissolved in the solvent is precipitated out. This process is called the gas antisolvent process (GAS), which exhibits some interesting technical and economic advantages. To date, the GAS process has been successfully used in recrystallization of organic solids,[7] fractionation of natural products,[8] and preparation of ultrafine particles,[9−20] including polymer microparticles.[12−20]

So far, many GAS processes have been investigated, but the focus is mainly on the process parameters effects on the properties of the products, and it has been known that particle shape, size distribution, and the morphology can be tuned by pressure, temperature, concentration of the solutes, etc. We are very interested in the effects of gas antisolvent on the polymer conformation, which are important to both pure and applied sciences.

Up to now, different researchers have studied the conformation of polymers in liquid solvents in the absence of gas antisolvent, and some interesting results have been obtained. For example, it has been found by light scattering and neutron scattering that the configuration of polymer chain depends on solvent quality; i.e., they are random coil in good solvent and rodlike aggregates in poor solvent.[21] Small-angle X-ray scattering (SAXS) method allows the elucidation of the size and the shape of polymer chain in liquid solutions.[22−27] Previous SAXS studies of supercritical fluids have also demonstrated that it is a powerful technique to describe structural information for the determination of the molecular structure of pure and modified supercritical systems.[28−31] In this work, we report the first application of SAXS technique to the study of the conformation of polymer chain in the solution in the presence of a gas antisolvent. The corresponding phase behavior of CO_2 + THF + PS ternary system was also studied.

Experimental Section

Materials. CO_2 (>99.995% purity) was provided by Analysis Instrument Factory of Beijing. Polystyrene (PS) ($M_w = 7.8 \times 10^4$, $M_w/M_n = 1.10$) was supplied by Polymer Laboratory, Institute of Chemistry, Chinese Academy of Sciences. THF (A. R. grade) was produced by Beijing Chemical Factory. The PS solutions with concentrations of 6.74×10^{-4}−8.36×10^{-3} g/cm^3 were made by the gravimetric method.

Apparatus and Procedures for Phase Behavior. The apparatus for measuring volume expansion and cloud points of CO_2 + THF + PS system consisted mainly of a 30 mL optical stainless steel cell, a magnetic stirrer, a constant temperature water bath, a pressure gauge, a gas cylinder, and a high-pressure pump. The accuracy of the pressure gauge, which was composed of a transducer (FOXBORO/ICT) and an indicator, was ±0.02 MPa in the pressure range 0−20 MPa. The temperature of the water bath was controlled by a HAAKE F3 controller. The temperature was determined using a platinum resistance thermometer (Beijing Chaoyang Automatic Instrument Factory, XMT) with an accuracy of ±0.1 K.

In a typical experiment, a suitable amount of PS/THF solution was loaded into the optical cell, and the cell was stabilized at the desired temperature. CO_2 was charged into the cell using the high-pressure pump until suitable pressure was reached. The stirrer was started. At the beginning, the pressure decreased and the volume of the liquid increased with time because of the dissolution of CO_2. The pressure remained constant with time when equilibrium was reached. The volume at equilibrium condition was known by reading the graduations on the cell. Some polymer molecules precipitated when the equilibrium pressure was high enough, which could be seen clearly through the windows of the optical cell. The cloud pressure, which was defined as the pressure at which the polymer begins to precipitate, was determined.

SAXS Experiments. The apparatus for the SAXS study was similar to the apparatus of on-line FT-IR measurement

[†] Institute of Chemistry.
[‡] Institute of High Energy Physics.
* To whom the correspondence should be addressed: E-mail hanbx@pplas.icas.ac.cn; Tel (8610)-62562821; Fax (8610)-62559373.

10.1021/ma000850z CCC: $19.00
Published on Web 09/28/2000

which was described in detail previously.[32] Briefly, the apparatus was consisted mainly of a gas cylinder, a high-pressure pump, a digital pressure gauge, a high-pressure SAXS cell, a thermometer temperature controller, and valves and fittings of different kinds. The pressure gauge as described above consisted of a transducer (FOXBORO/ICT) and an indicator. The temperature-controlled SAXS cell was composed mainly of a stainless steel body and two diamond windows of 8 mm in diameter and 0.4 mm in thickness. Diamond is an excellent window material for SAXS studies because it has low absorbance and low scattering power. The cell body was coiled with an electric heater and a heat-insulated ribbon outside. The insulated cell was electrically heated to ±0.2 K of the desired temperature by using a temperature controller with a platinum resistance temperature probe (model XMT, produced by Beijing Chaoyang Automatic Instrument Factory). The X-ray path length of the cell was 1.5 mm, and the internal volume of the cell was 2.7 cm^3. There was a small magnetic stirrer in the cell to stir the fluids before the SAXS measurements, so that the equilibrium could be reached in a shorter period of time.

SAXS experiments were carried out at Beamline 4B9A at the Beijing Synchrotron Radiation Facility, using a SAXS apparatus constructed at the station. A detailed description of the spectrometer is given elsewhere.[33] The detector can be translated along the vertical and horizontal axes in a range of 30 mm with a precision of 10 μm. The experiments had an angular resolution of better than 0.5 mrad with this setting. The data accumulation time was 3 min. The angular range was chosen so as to provide data from $h = 0.005$ A^{-1} to $h = 0.15$ A^{-1}, where the magnitude of scattering vector $h = 2\pi \sin \theta/\lambda$, θ and λ being respectively the scattering angle and incident X-ray wavelength of 1.54 Å. The distance between the sample chamber and the detector was 1.52 m. Background scattering from the slit collimator, the solvent, and the residual air path between the vacuum chamber and the detector was measured. Excess SAXS scattering from PS solute was corrected for incident beam decay sample thickness and transmission. The background scattering was also subtracted.

Before the experiment, the SAXS cell was flushed with CO_2, and then a suitable amount of PS/THF solution was filled into the cell. CO_2 was charged into the cell with stirring at the temperature of interesting. The cell was connected to the apparatus after the equilibrium was reached, and the X-ray scattering was recorded.

Results and Discussion

Phase behavior. The volume expansion of the solution was determined at 298.15, 308.15, 318.15, and 328.15 K and at different pressures.

The cloud pressure at different temperature was also determined. As an example, Figure 1 shows the volume expansion (V_e) plots of the CO_2 + THF + PS system at 308.15 K and at different solution concentrations. The volume expansion is defined by the following equation:

$$\text{volume expansion } (V_e) = (V - V_o)/V_o \qquad (1)$$

where V_o and V stand for the volume of the CO_2-free liquid solution and CO_2-saturated liquid solution. The volume expansion (V_e) experiments were repeated at least three times for each equilibrium condition, and the reproducibility was better than ±1%. It was estimated that the accuracy of the measurements was better than ±2%.

Figure 2 shows cloud pressure (P_c) at different temperatures and various PS concentrations. As expected, the volume expansion and cloud pressure decrease with the original concentration of PS. The data of volume expansion and cloud point allowed us to determine how much solution should be charged into the SAXS cell at different temperatures and pressures and what conditions we need to choose to investigate the conformation of PS chain.

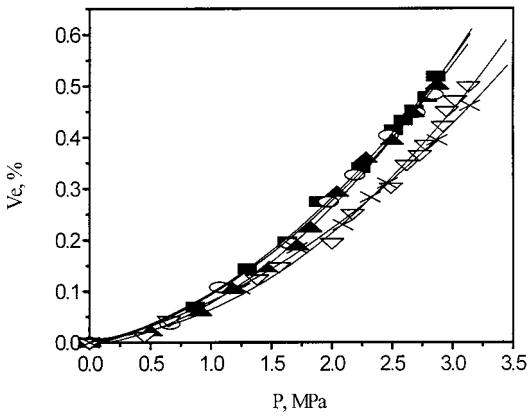

Figure 1. Volume expansion (V_e) of PS/THF solutions at 308.15 K.

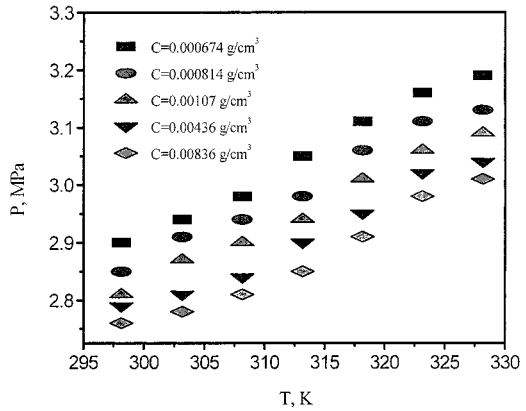

Figure 2. Cloud point pressure (P_c) of PS/THF solutions at different temperatures.

SAXS Study. Data Processing. We are interested in the conformation of PS chain in solution in the course of adding antisolvent CO_2. Its scattering curve was obtained by subtracting the scattering of the solvent + antisolvent from the scattering of the solution.

The scattering intensities $I_{exp}(h,C)$ measured as a function of momentum transfer h and polymer concentration C of the polymer, usually expressed in g/cm^3, may be treated according to Zimm, Flory, and Bouche:[34]

$$\frac{KC}{I_{exp}(h,C)} = \frac{1}{M_w I_n(h)} + 2A_2 Q(h)C + \ldots \qquad (2)$$

where K is the optical constant, A_2 is the second virial coefficient, M_w is molecular weight of the dissolved polymer, and $I_n(h)$ is the single particle scattering function. $Q(h)$ and $I_n(h)$ are normalized in such a way that $I_n(0) = 1$ and $Q(0) = 1$. The first term on the right side of eq 2 is merely due to intramolecular interference, whereas the higher term reflects the influence of the intermolecular interference.

From eq 2, if $h \to 0$, we can also obtain the equation[34]

$$\lim_{h\to 0} \frac{KC}{I_{exp}(h,C)} = \frac{1}{M}(1 + 2A_2 MC + \ldots) \qquad (3)$$

from which the thermodynamic analysis of the dilute system can be performed. If $C \to 0$, we can obtain the equation[34]

$$\lim_{c\to 0}\frac{KC}{I_{exp}(h,C)}=\frac{1}{MI_n(h)}=\frac{1}{M}\left(1+\frac{\langle R^2\rangle}{3}h^2+...\right) \quad (4)$$

which contains all information on the shape and the conformation of the isolated macromolecules in solution. The initial slopes of eq 3 vs C and eq 4 vs h^2 yield the second virial constant A_2 and mean-square radius of gyration $\langle R_g^2\rangle^{1/2}$, respectively.[34] To a first approximation, we only consider the first two terms on the right side in eq 2. At the angle of $h = 0$, from eq 2, we have

$$\frac{KC}{I_{exp}(0,C)}=\frac{1}{M}+2A_2C \quad (5)$$

or

$$\frac{1}{MC}=-2A_2+\frac{K}{I_{exp}(0,C)} \quad (6)$$

Thus, K and A_2 can be obtained from the slope and intercept of $1/MC$ vs $1/I_{exp}(0,C)$ plot, as can be known from eq 6.

The PS concentration changed with antisolvent pressure because the volume expansion is a function of pressure as shown in Figure 1. The concentration after expansion should be used, which could be easily obtained from original (CO_2-free) PS concentration and the volume expansion determined in this work as shown in Figure 1.

Scattering Curve. In this work, we determined scattering intensity at PS concentrations of 6.74×10^{-4}, 8.14×10^{-4}, 1.07×10^{-3}, 4.36×10^{-3}, and 8.36×10^{-3} g/cm^3 at different pressures. As an example, Figure 3 shows the log−log plot of I vs h at $C = 6.74 \times 10^{-4}$ g/cm^3 and at different pressures. I is the excess scattering intensity due to the PS solute.

The scattering intensity increases with pressure at pressures lower than the cloud pressure. We have known that the X-ray scattering is due to the contrast provided by the difference in electron densities in the solute and solvent. The presence of CO_2 in the system creates more and more large difference in electron between the solute on one hand and solvent on the other. Another feature of SAXS profiles is that the scattering intensity at the pressure higher than cloud pressure decreases considerably. It may result from the precipitation of some PS in the solution because the pressure is higher than the cloud pressure. The precipitated PS dropped below the irradiated volume.

Figure 4 shows log−log plot of I vs h for different PS concentration at 1.5 MPa. The magnitude of the concentration effect depends on the shape and charge of the particle and the solvent. No general function exists which would allow prediction of the magnitude of the concentration effect. From Figure 4, we can say that concentration has large effect on the scattering of polymer solution.

Second Virial Constant A_2. To use eq 6 to get A_2 and K, the scattering intensity plots of $I_{exp}(h,C)$ vs h at different concentrations were obtained using the experimental data. The data were extrapolated to $h = 0$, and the values of $I_{exp}(0,C)$ were obtained. Figure 5 shows the $1/M_wC$ vs $I_{exp}(0,C)$ curves, which are linear in the concentration range studied in this work. This verifies that we can get reliable results although we only considered the first two terms on the right side of eq 2. Thus, K and A_2 at different concentrations were easily obtained from slope and intercept of $1/M_wC$ vs $I_{exp}(0,C)$ curves, and the results are listed in Table 1.

The second virial constant A_2 is related with the solvent power of the solvent for the polymer. As expected, A_2 depends on the pressure or the volume

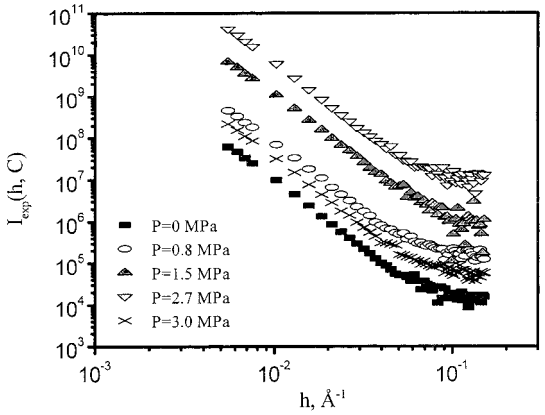

Figure 3. SAXS profiles of PS in THF at 308.15 K and different pressures with PS/THF concentration of 6.74×10^{-4} g/cm^3.

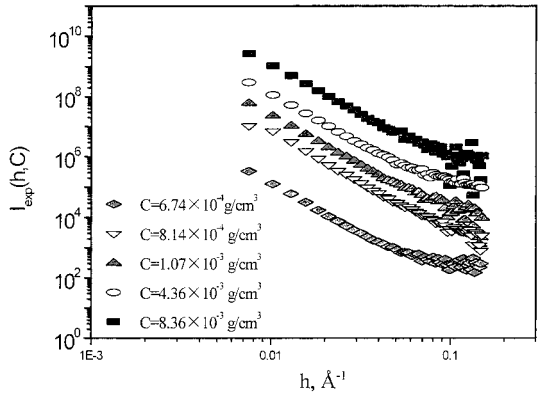

Figure 4. SAXS profiles of PS in THF at 308.15 K and 1.5 MPa with different PS concentrations.

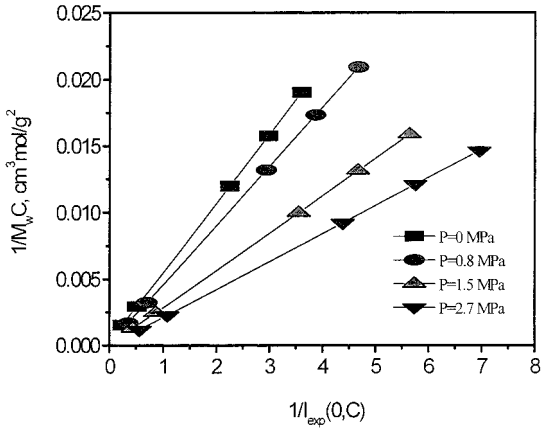

Figure 5. $1/M_wC$ vs $1/I_{exp}(0,C)$ plots at different pressures to obtain K and A_2.

Table 1. Values of K, A_2, and Radius of Gyration of PS at Different Pressures

press. (MPa)	K (cm^3 mol/g^2)	A_2 (cm^3 mol/g^2) × 10^3	$\langle R_g^2\rangle^{1/2}$ (Å)
0	52.05	0.13	140.1
0.8	44.44	0.065	127.0
1.5	40.36	0.030	117.4
2.7	35.59	−0.0025	105.3

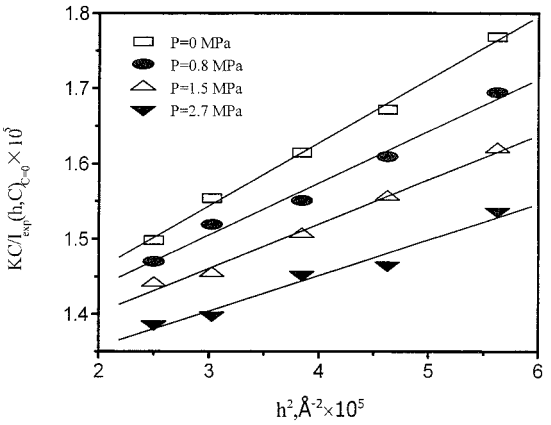

Figure 6. Plots of $KC/I_{exp}(h,C)_{C=0}$ against of h^2 for the PS in THF at 308.15 K and different pressures.

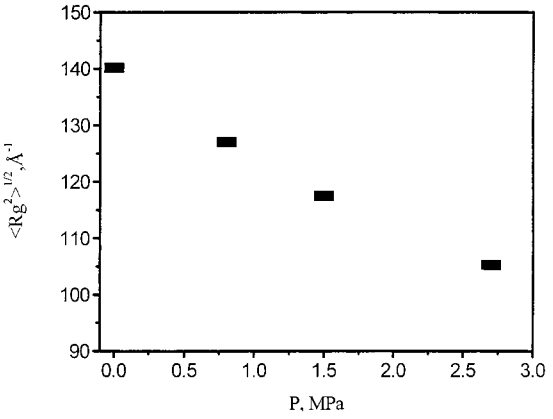

Figure 7. Effect of pressure on the $\langle R_g^2\rangle^{1/2}$ for the PS in THF at 308.15 K.

expansion. A_2 changes from positive to negative with increasing pressure. This means that the soluble ability of THF to PS is decreasing with adding of antisolvent CO_2.

Mean-Square Radius of Gyration. To calculate the mean-square radius of gyration $\langle R_g^2\rangle^{1/2}$ using eq 4, the data for $KC/I_{exp}(h,C)_{C=0}$ are required. To do this, $KC/I_{exp}(h,C)$ is plotted against C. The values of K in Table 1 were used in the calculation. $KC/I_{exp}(h,C)$ vs C curves were extrapolated to zero concentration, and $KC/I_{exp}(h,C)_{C=0}$ was obtained.

$KC/I_{exp}(h,C)_{C=0}$ vs h^2 curves are linear in Figure 6. Thus, $\langle R_g^2\rangle^{1/2}$ can be evaluated from their slopes, and the values of $\langle R_g^2\rangle^{1/2}$ are also shown in Table 1.

Figure 7 shows the dependence of $\langle R_g^2\rangle^{1/2}$ on pressure. It is well-known that $\langle R_g^2\rangle^{1/2}$ is related to the conformation of the polymer molecules. The value becomes larger when the molecules is expanded. It can be seen from Figure 7 that $\langle R_g^2\rangle^{1/2}$ decreases with increasing pressure. It indicates that the PS chain experiences shrinking in the course of adding antisolvent CO_2. THF is a good solvent for PS and the coil expanded due to prevailing intersegmental repulsion; after adding CO_2, the solvent power of THF is reduced, and PS chain shrunk due to prevailing intersegmental attraction.

Acknowledgment. This work was supported by the National Basic Research Project-Macromolecular Condensed State and the National Natural Science Foundation of China (29633020, 29725308).

References and Notes

(1) McHugh, M. A.; Krukonis, V. J. *Supercritical Fluids Extraction Principles and Prantice*, 2nd ed.; Butterworth-Heinemann: Stoneham, MA, 1994; p 189.
(2) Tuminello, W.; Dee, G. T.; McHugh, M. A. *Macromolecules* **1995**, *28*, 1506.
(3) Mertsch, R.; Wolf, B. A. *Macromolecules* **1994**, *27*, 3289.
(4) Zhao, X.; Watkins, R.; Batron, S. W. *J. Appl. Polym. Sci.* **1995**, *55*, 773.
(5) Xiong, Y.; Kiran, E. *Polymer* **1995**, *36*, 4817.
(6) Kordikowski, A.; Schenk, A. P.; Van Nielen, R. M.; Peters, C. J. *J. Supercrit. Fluids* **1995**, *8*, 205.
(7) Gallagher, P. M.; Coffey, M. P.; Krukonis, V. J. *J. Supercrit. Fluids* **1992**, *5*, 130.
(8) Catchpole, O. J.; Hochmann, S.; Anderson, S. R. J. *High Pressure Chem. Eng.* **1996**, 309.
(9) Reverchon, E.; Della Porta, G.; Sannino, D.; Ciambelli, P. *Powder Technol.* **1999**, *102*, 127.
(10) Reverchon, E. *J. Supercrit. Fluids* **1999**, *15*, 1.
(11) Chang, C. J.; Randolph, A. D. *AIChE J.* **1990**, *36*, 939.
(12) Dixon, D. J.; Johnston, K. P.; Bodmeier, R. A. *AIChE J.* **1993**, *39*, 127.
(13) Dixon, D. J.; Johnston, K. P. *J. Appl. Polym. Sci.* **1993**, *50*, 1929.
(14) Lele, A.; Shine, A. D. *AIChE J.* **1992**, *38*, 742.
(15) Mawson, S.; Johnston, K. P.; Betts, D. E.; McClain, J. B.; DeSimone, J. M. *Macromolecules* **1997**, *30*, 71.
(16) Luna-Barcenas, G.; Kanakia, S. K.; Sanchez, I. C.; Johnston, K. P. *Polymer* **1995**, *36*, 3173.
(17) Yeo, S.-D.; Debenedetti, P. G.; Radosz, M.; Giesa, R.; Schmidt, H.-W. *Macromolecules* **1995**, *28*, 1316.
(18) Yeo, S.-D.; Debenedetti, P. G.; Radosz, M.; Schmidt, H.-W. *Macromolecules* **1993**, *26*, 6207.
(19) Dixon, D. J.; Luna-Barcenas, G.; Johnston, K. P. *Polymer* **1994**, *35*, 3998.
(20) Luna-Barcenas, G.; Kanakia, S. K.; Sanchez. I. C.; Johnston, K. P. *Polymer* **1995**, *36*, 3173.
(21) Tompa, H. *Polymer Solution*; Academic Press: New York, 1956; p 297.
(22) McClain, J. B.; Londino, D.; Combes, J. R.; Romack, T. J.; Canelas, D. A.; Betts, D. E.; Wignall, G. D.; Samulski, E. T.; DeSimone, J. M. *J. Am. Chem. Soc.* **1996**, *118*, 917.
(23) Hayashi, H.; Hamada, F.; Nakajima, A. *Macromolecules* **1974**, *7*, 959.
(24) Fujiwara, Y.; Flory, P. J. *Macromolecules* **1970**, *3*, 288.
(25) Yoon, D. Y.; Flory, P. J. *Macromolecules* **1976**, *9*, 294.
(26) Hyman, A. S. *Macromolecules* **1975**, *8*, 849.
(27) Smith, T.; Carpenter, D. K. *Macromolecules* **1968**, *1*, 204.
(28) Londono, J. D.; Dhramapurikar, R.; Cochran, H. D.; Wignall, G. D.; McClain, J. B.; Betts, D. E.; Canelas, D. A.; DeSimone, J. M.; Samulski, E. T.; Chillura-martino, D.; Triolo, R. *J. Appl. Crystallogr.* **1997**, *30*, 690.
(29) Nishikawa, K.; Tanaka, I. *Chem. Phys. Lett.* **1995**, *244*, 149.
(30) Nishikawa, K.; Tanaka, I.; Amemiya, Y. *J. Phys. Chem.* **1996**, *100*, 418.
(31) Pfund, D. M.; Zemanian, T. S.; Lineham, J. C.; Fulton, J. L.; Yonker, C. R. *J. Phys. Chem.* **1994**, *98*, 11846.
(32) Lu, J.; Han, B. X.; Yan, H. K. *Phys. Chem. Chem. Phys.* **1999**, *1*, 449.
(33) Dong, B. Z.; Sheng, W. J.; Yang, H. L.; Zhang, Z. J. *J. Appl. Crystallogr.* **1997**, *30*, 877.
(34) Glatter, G.; Krathy, O. *Small-Angle X-ray Scattering*; Academic Press: London, 1982; p 387.

MA000850Z